Pergamon

Applied Thermal Engineering Vol. 18, No. 6, pp. 481–489, 1998

Printed in Great Britain
PII: S1359-4311(97)00044-6
1359-4311/98 $19.00 + 0.00

EXPERIMENTAL VERIFICATION AND CALIBRATION OF THE BLOW-OFF HEAT FLUX SENSOR

N. Martins,* M. G. Carvalho,* N. H. Afgan* and A. I. Leontiev†

*Instituto Superior Técnico, Av. Rovisco Pais, Pavilhão Máquinas, Piso 1, 1096 Lisboa Codex, Portugal; and †Moscow Technical University, Moscow, Russia

(*Received* 26 *September* 1996)

Abstract—A new heat flux meter to assess the total hemispherical radiation heat flux using the emperature distribution in a porous media crossed by a cooling gas stream is discussed. The paper presents calibration data based on the experimental measurement of the temperature distribution in the porous sensing element. A calibration furnace (black body) was used as radiation source and pressurised air (2 bar) was used as cooling gas. The porous specimen, a sintered stainless steel disc, was placed in the instrument head with the possibility to control the air mass flow rate. The sensing element was filled with shielded ungrounded thermocouples positioned in well-defined locations in order to determine the axial temperature distribution in the porous disc. The measurements were performed for the experimental regimes corresponding to the thermal radiation heat flux levels in the range of 40–150 kW/m^2.

A linear calibration curve was obtained for the different air mass flow rates. It was shown that by adjusting the gas mass flow rate through the porous sensing element it is possible to control its temperature distribution and the relative importance of radial conduction losses in the sensing element.

Keywords—Heat flux sensor, experimental verification, calibration, industrial application.

NOMENCLATURE

A_{sp}	specific surface	(m^{-2} m^{-3})
BOG	Blow Off Gas	
c_p	specific heat of gas	(J kg^{-1} K^{-1})
D	sensing element diameter	(m)
dp	pores average diameter	(m)
Err	instrument error	(percentage)
L	sensing element thickness	(m)
$\dot{m}$	blow-off mass flow rate	(kg s^{-1})
q	heat flux	(W m^{-2})
SLPM	standard litres per minute	
T	temperature	(°C)

Greek letters

Δ	difference	
ε	emissivity	
σ	Boltzman constant	($5.57 \cdot 10^{-8}$ W m^{-2} T^{-4})

Subscripts

app	apparent
ax	axial
cool	cooling system
in	inlet of the porous disc
loss	losses
out	outlet of the porous disc
r	radial
SP	set-point
isol	isolation ring

INTRODUCTION

Thermal radiation is an important parameter for the diagnosis of a number of systems. Boilers, furnaces, combustion chambers are among those systems where one of the most important parameters to be determined is the thermal flux at the respective walls or charge.

A number of attempts have been made to develop instruments able to perform heat flux measurements in thermal equipment for industry. This is a problem of substantial interest for many industrial processes [1–4]. With different success, most of the methods have been used in the control and diagnostics of those systems [5], however there are different limitations observed for each of the specific instrument designs. For this reason, the development of a new heat flux measurement method is a challenging work. In particular, the thermal radiation flux measurement in hostile environments is needed to meet the requirements of the respective diagnostic systems. The instrument for the thermal hemispherical radiation flux measurement [6] is based on the determination of the temperature difference of the gas flowing through a porous disc exposed to the particular heat flux to be measured.

The gas stream has an essential effect on the method since its purpose is:

—To cool the instrument sensible surface,
—To avoid the possibility of fouling on the sensible surface,
—To make it possible to distinguish between the radiation and convection components of the total hemispherical heat flux, and
—To adjust the instrument range to the heat flux level to be measured.

The gas stream acts to blow-off the boundary layer from the sensor surface. The boundary layer on the sensor surface is blown off by a critical gas stream [7]. If an over-critical blow-off mass flow rate is imposed, the convection component of the total heat flux is zero. If a sub-critical blow-off mass flow rate is considered, the incident heat flux presents the two components, Fig. 1. A sequence of two measurements is enough to gather the required data to determine the radiation and convection components of the total heat flux. The heat transfer characteristic of the porous matrix and the associated fluid flow have to be selected to meet the requirements posed by the instrument concerning its accuracy and material limitations. The design of the instrument was assisted by the mathematical modelling of the heat and mass transfer in the porous sensing element [8]. The 2D analysis of the instrument, based on the numerical solution of the transport equations for the porous matrix and BOG, has shown that it is possible to obtain well defined design parameters under the selection criteria applied, resulting in the present sensor design. A scheme of the proposed instrument head is shown in [8].

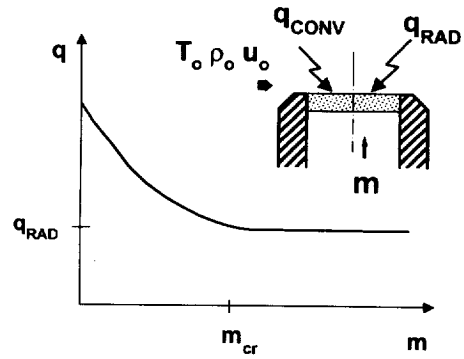

$$m_{cr} = C \frac{\rho_o u_o}{\sqrt{Re_o}}$$

Fig. 1. Working principle.

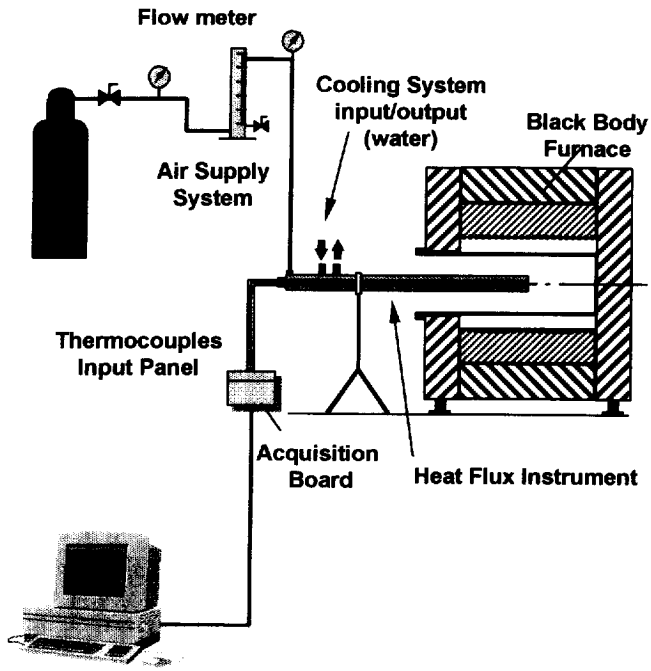

Fig. 2. Experimental set-up.

EXPERIMENTAL SET-UP

The experimental apparatus, Fig. 2, consists of a *black body furnace* acting as radiation source, a *heat flux meter prototype* with the respective cooling system, an *air supply system* and a *data acquisition system*. A short description of the various systems is given below.

The radiation heat source

The radiation source is an Isothermal Technology Limited high temperature furnace, model ITL-M-17702. The black body radiator is a cylindrical sodium heat pipe, heated-up by electric resistances. The radiating cavity can be considered as a black body radiator due to its aspect ratio and the high uniformity of the surface temperature. This kind of furnace presents a high stability and spatial homogeneity of the temperature because of its working principle (phase change). The furnace resolution is 0.1°C.

The radiating cavity temperature was verified with a type S thermocouple and compared with the set point temperature. The greatest deviation between these temperatures was 0.15%, corresponding to a furnace error of 0.6% in heat flux units.

The heat flux sensor prototype

A porous element, a stainless steel protection net, a Teflon® isolation ring, three type K thermocouples, a porous specimen holder and a water cooling system basically comprise the developed heat flux sensor.

The porous element is a sintered stainless steel (AISI 316) disc with 56% open porosity, 9 mm diameter and 4 mm thickness. In order to increase its emissivity an oxidisation procedure, involving keeping its temperature at 850°C for approximately 12 h was performed resulting in a uniform matt black colour for the whole surface.

A stainless steel mesh made of 0.036 mm wires with 325 pores per linear inch was also oxidised following a procedure similar to that described above.

To measure the temperature distribution in the porous element three miniature ungrounded thermocouple probes from Omega Engineering Inc., Stamford, CT were used. The probes were placed according to Fig. 3 and are type K thermocouples within an inconel sheath with an external diameter of 0.254 mm.

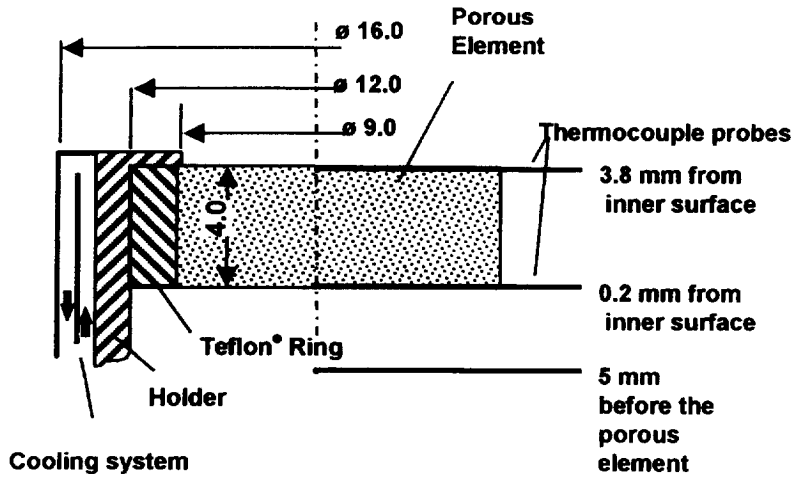

Fig. 3. Sensing element.

The porous element surface to be exposed to the heat flux was covered by a protective stainless steel mesh. The whole set was held in a water cooled stainless steel cylindrical body with an external diameter of 28 mm and 500 mm length, Fig. 4.

The acquisition system

The outputs of the thermocouples were read using an OMD-5508TC board from Omega Engineering Inc., Stamford, CT and Labtech Notebook for Windows acquisition software installed in a 486 IBM compatible PC. The output indicates the furnace set point, the respective heat flux, the temperature of the air stream at the inlet port, the temperature of the thermocouples inside the porous media and the difference between the relevant temperatures.

Air supply system

The blow-off gas used in the present experiment was pressurised air. The supply pressure was fixed at 2 bar and the air mass flow rate was measured and controlled *via* a Fisher and Porter variable area rotameter with a maximum output of 17 SLPM of air. The rotameter used pre-

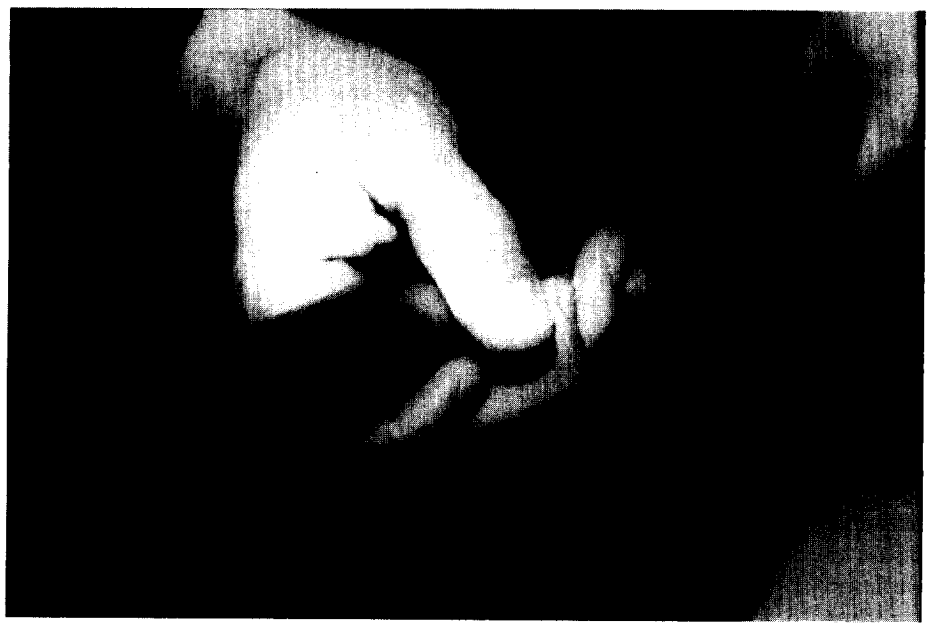

Fig. 4. Instrument prototype.

Table 1. Values of the calibration furnace temperature and the respective BOG mass flow rates

Set-point [°C]	Heat flux [kW/m²]	Blow-off mass flow rate [SLPM]										
650.0	41.2	1,2	2,5	3,8	5,2	6,7	8,3	10,0	12,2	14,0	15,9	
750.0	62.1	1,2	1,8	3,1	4,5	6,0	7,5	9,1	10,9	12,8	15,9	
800.0	75.2	1,2	2,5	3,8	5.4	6,7	8,3	10,0	11,8	13,8	15,9	
850.0	90.2	1,2	2,5	3,8	5,2	6,7	8,3	10,0	11,8	13,8	15,9	
900.0	107.4	1,2	1,8	3,1	4,5	6,1	7,5	9,1	10,9	12,8	14,8	15,9
950.0	126.9	1,2	2,5	2,5	4,0	5,2	617	8,3	9,8	11,8	13,8	15,9
1000.0	149.0	1,2	1,2	1,8	3,1	4,5	6,0	7,5	9,1	10,9	12,8	14,8	15,9

sents a repeatability of 0.5% of full-scale reading and a standard accuracy class of 4 according to VDE/VD13513. The air pressure is monitored before and after the rotameter to calculate the air mass flow rate. The air temperature at the inlet port of the instrument body was measured with a type K thermocouple.

EXPERIMENTAL PROCEDURE

During the setting up of the experiment, special care was required in order to reduce the noise during the thermocouple readings due to the low temperature levels to be measured. For that purpose, sheathed thermocouples were used and the sheaths were connected to a common earth. The temperature readings were made with a sampling rate of 60 Hz and averaged for each second.

The radiation heat source was heated up to the first set point and stayed at that temperature until a stable temperature level was attained. The blow-off air mass flow rate was set to the appropriate level. The heat flux meter was then introduced into the radiating cavity at a depth such that the heat flux stabilises at the highest level in order to avoid edge effects from the furnace cavity. The temperature evolution was continuously monitored *via* the acquisition system and when transient effects were not present, the temperature readings from the thermocouples were taken. For each temperature level of the furnace, different blow-off gas mass flow rates were considered and the corresponding temperatures of the thermocouples read. The values of the calibration furnace temperature and the respective BOG mass flow rates are summarised in Table 1.

RESULTS AND DISCUSSION

For the above-described testing conditions, three different temperatures were measured. The location of the respective thermocouples is shown in Fig. 3. In addition, the cooling water temperature was also measured. These data were used to perform an energy balance on the porous sensing element in order to verify the instrument linearity and accuracy over the range of use.

Important parameters and equations

The relevant heat transfer mechanisms and associated parameters are presented in Fig. 5. Only a fraction of the incident radiative heat flux, q_R, is transferred to the solid phase of the porous sensing element. That fraction is determined by the apparent emissivity of the porous surface, ε_{app}. It will be transported by radial conduction through the solid phase to the cooling system, q_{loss}, and by convection to the BOG stream flowing through the porous specimen, resulting in an axial temperature difference, ΔT_{ax}. The temperature difference between the solid matrix and the BOG is neglected due to the high specific surface of the porous disc.

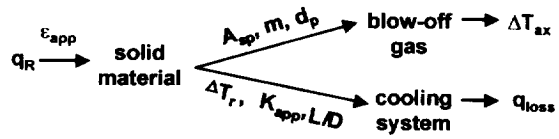

Fig. 5. Heat transfer mechanisms and important parameters.

The controlling parameters for energy that is lost by radial conduction are: the effective conductivity of the porous disc; its thickness/diameter ratio and the radial temperature gradient.

The energy given to the blow-off gas stream is a function of the specific surface of the porous media, the diameter of the pores and the blow-off gas mass flow rate. However, the controlling parameter for the heat flux and mass flow levels considered is the specific surface, which makes the temperature difference between the porous media and the BOG negligible, for all the conditions studied.

Considering the heat and mass transfer model described above an energy balance to the porous disc yields the following calibration equation:

$$q_{\text{cal}} = \frac{4\dot{m}c_{\text{p}}}{\varepsilon_{\text{app}}\pi D^2}(T_{\text{out}} - T_{\text{in}}) + \frac{4L}{\varepsilon_{\text{app}}D}q_{\text{loss}} \tag{1}$$

where the first term on the right side represents the energy gain by the blow-off gas and the second term represents the radial heat losses to the cooling system.

In the above equation the unknowns are the heat flux, q, the apparent emissivity, ε_{app}, and the radial heat losses, q_{loss}. However, if the blow off mass flow rate is sufficiently high it will be shown that the radial losses became negligible and Equation (1) can be simplified to:

$$q_{\text{cal}} = \frac{4\dot{m}c_{\text{p}}}{\varepsilon_{\text{app}}\pi D^2}(T_{\text{out}} - T_{\text{in}}). \tag{2}$$

The apparent emissivity is assumed constant and can be determined as will be explained later and Equation (2) can then be used to calculate the radiative heat flux. The radiative heat flux from the calibration furnace is given by:

$$q_{\text{SP}} = \sigma T_{\text{SP}}^4. \tag{3}$$

In addition, the instrument accuracy is determined by the following error expression:

$$Err = \frac{|q_{\text{cal}} - q_{\text{SP}}|}{q_{\text{SP}}}100. \tag{4}$$

The two parameters to be estimated are the apparent emissivity of the sensing element and the minimum flow rate level required to make the radial losses negligible. These two parameters can be obtained simultaneously as follows.

By definition, it may be written that the radiative emissivity of a grey surface is given by the ratio of the radiative energy absorbed by the surface and the incident radiative energy. The same concept will be taken here for the apparent emissivity. For the present application, the absorbed energy is totally transferred to the BOG and, if the radial losses are negligible, is given by Equation (2). The incident radiative flux is that emitted by the calibration furnace, given by Equation (3). Making the corresponding substitutions the apparent emissivity is given by:

$$\varepsilon_{\text{app}} = \frac{4\dot{m}c_{\text{p}}}{\pi D^2 \sigma T_{\text{SP}}^4}(T_{\text{out}} - T_{\text{in}}) \tag{5}$$

where all the variables are known.

However, Equation (5) is valid only under the following assumptions:

1. For the considered temperature range, the apparent emissivity and the specific heat of the BOG are constant.
2. The radial losses are negligible.
3. The temperature distribution is constant at the inlet and outlet of the porous media.
4. The sensing element surface can be considered grey.

Plotting the emissivity calculated by Equation (4) against the BOG mass flow rate, Fig. 6, two important parameters can be obtained. The first is the minimum BOG mass flow rate that makes negligible the radial losses. Actually as the BOG mass flow rate increases the determined emissivity tends to a constant value, which is obtained at $\dot{m} \geq 7.5$ SLPM with an error of $\pm 5\%$.

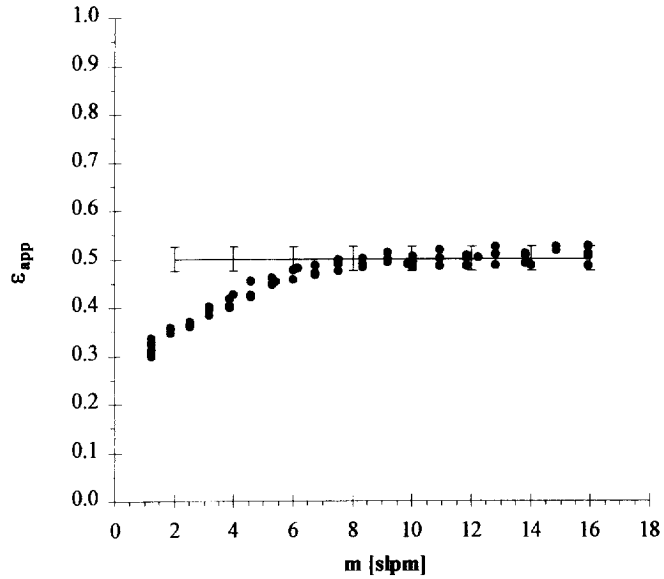

Fig. 6. Apparent emissivity and minimum BOG mass flow rate determination.

The second is the apparent emissivity, determined under the conditions described above which is $\varepsilon_{app} = 0.50 \pm 5\%$. This value is used as a constant in Equation (2).

Calibration curve and accuracy

All the parameters to be defined in order to make it possible to use Equation (2) as a calibration expression for the heat flux sensor are now available. For the tested design, the incident hemispherical radiation flux can be determined by Equation (6), resulting from the substitution of all the constant parameters in Equation (2). The heat flux can be directly calculated by measuring the temperature difference and the corresponding BOG mass flow rate.

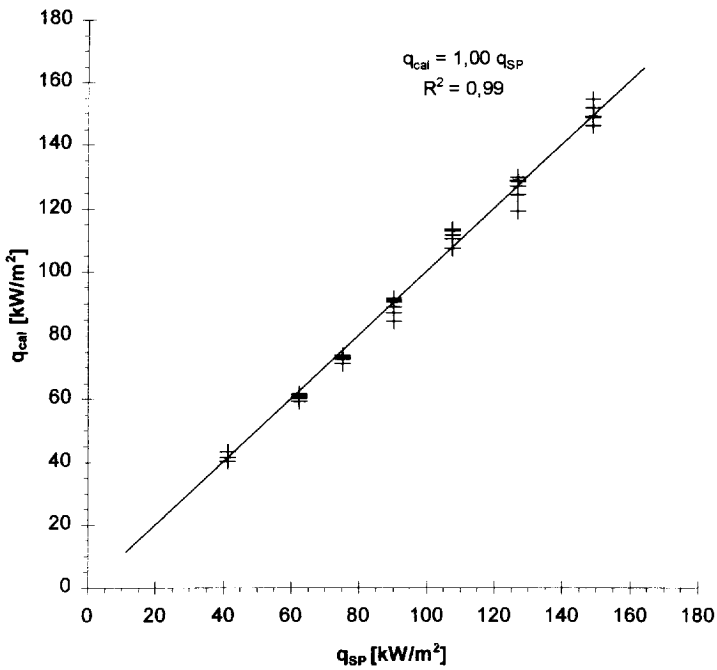

Fig. 7. Instrument performance. Comparison of measured data with reference data.

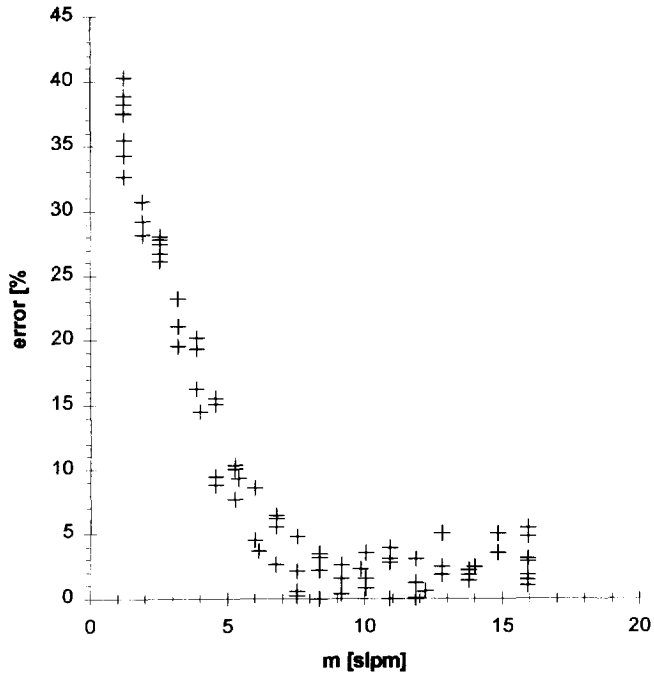

Fig. 8. Instrument accuracy as a function of BOG mass flow rate.

$$q = \vartheta \dot{m}(T_{\text{out}} - T_{\text{in}}) \tag{6}$$

with $\vartheta = 682.76[\frac{\text{W}}{\text{SLPM m}^2\ ^\circ\text{C}}]$.

In Fig. 7, the heat flux determined using Equation (6) is plotted against the corresponding calibration heat flux from the calibration furnace (reference value). The agreement between the data is good with respect to linearity and shift at zero, presenting an error always less than $\pm 5\%$ for the studied range. The respective linear regression line shows the good agreement between the calculated and the reference heat flux. The accuracy of the instrument is defined by the error determined using Equation (4). Figure 8 shows the calculated error for all the tested operating

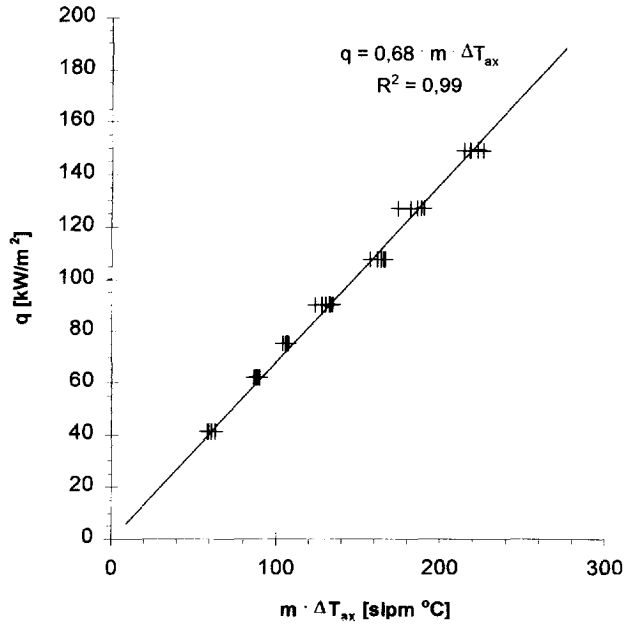

Fig. 9. Calibration curve.

conditions as a function of the blow-off mass flow rate. Nevertheless, the large errors obtained for low BOG mass flow rates due to radial loss effects are lower than 5% for mass flow rates higher than 7.5 SLPM.

Figure 9 shows a practical calibration curve to be used when operating the instrument relating the measured quantities and the required heat flux.

CONCLUSIONS

Calibration data for a new heat flux instrument based on experimental measurement of the temperature distribution in a porous disc crossed by an air stream have been presented. The ranges considered were 40–150 kW/m^2 for the heat flux and 1.7–17.2 SLPM for the air mass flow rate.

A calibration equation taking into account the heat transfer to the blow-off was proposed and validated using experimental data. The effect of the radial losses on the instrument performance was analysed. A regime for the BOG mass flow that makes the radial loss effects negligible was identified. The apparent emissivity of the sensing porous disc was determined and used for calibration purposes. However, it should be stressed that this parameter is not a real physical property but a fitting parameter mathematically correlated with the corresponding property.

With the current design, it is possible to measure the hemispherical radiative heat flux with an error smaller than 5%. A well-defined range was found where the incident radiative heat flux is proportional to the axial temperature difference in the porous sensing element. This proportional range is defined by $\dot{m} \geq 7.5$ SLPM. The instrument range can be adjusted within a broad limit of the heat flux to be measured, without accuracy degradation, by adjusting the blow-off mass flow rate in order to operate in the proportional regime.

Acknowledgements—The authors would like to acknowledge I.P.Q. (the Portuguese Quality Institute) which allowed us to use their black body calibration facilities as well as Eng. M. Eduarda Filipe for the collaboration during the calibration procedures. This work was partially financed by the JOULE Programme (DG XII—European Commission).

REFERENCES

1. W. Clay, I. S. Davidson, Heat flux-meter in furnace boiler to monitor deposit. In *Proc. IMECO Symp. on Thermal and Temperature Measurements in Science and Industry, Liverpool, 1987*, pp. 345–357 (1987).
2. E. W. Northover, The CERL Dometer—A radiation heat flux on the tube metal for highly rated boiler. *CEGB Disclosure Bull.*, No. 294 (1987).
3. B. Brajuskovic, M. Matovic and N. Afgan, A heat flux-meter for ash deposit monitoring systems—1. Ash deposit prevention. *Int. J. Heat Mass Transfer* **34**(9), 2291–2303 (1991).
4. B. Brajuskovic and N. Afgan, A heat flux-meter for ash deposit monitoring systems—2. "Clean" flux-meter characteristics. *Int. J. Heat Mass Transfer* **34**(9), 2303–2315 (1991).
5. T. E. Diller, Advances in heat flux measurements, in *Advances in Heat Transfer*, Vol. 23, pp. 279–368. Academic Press (1993).
6. N. H. Afgan and A. I. Leontiev, Instrument for thermal radiation flux measurement in high temperature gas. *Heat Recovery Systems & CHP* **15**(4), 347–350 (1995).
7. A. I. Leontiev, Heat and mass transfer in turbulent boundary layers, in *Advances in Heat Transfer*, Vol. 3, pp. 33–100, Academic Press, New York (1966).
8. N. Martins *et al.*, A new instrument for radiation heat flux measurement—Analysis and parameter selection. *Heat Recovery Systems & CHP* **15**(8), 787–796 (1995).